AgriEngineering

MDPI

Article

Design and Experiment of a Double-Layer Orthogonal Photoelectric Through-Beam Detection Device for High-Throughput Wheat Seed Flow

Haojie Zhang [1], Bing Qi [1,*], Yunxia Wang [1,*], Shutong Huang [2], Youqiang Ding [1] and Wenyi Zhang [1]

[1] Nanjing Institute of Agricultural Mechanization, Ministry of Agriculture and Rural Affairs, Nanjing 210014, China; 821012430114@caas.cn (H.Z.); dingyouqiang@caas.cn (Y.D.); zwy-yxkj@163.com (W.Z.)
[2] College of Engineering, Northeast Agricultural University, Harbin 150030, China; 18262638256@163.com
* Correspondence: qb0823521@163.com (B.Q.); wangyunxia@caas.cn (Y.W.)

Abstract

Aiming at the problems of mutual overlapping in high-throughput seed flow and difficulty in accurate detection of seeding rate during high-speed precision wheat seeding, a double-layer orthogonal through-beam photoelectric detection device for high-throughput wheat seed flow was developed in this paper, based on a four-layer staggered hook-type precision wheat seed-metering device. Combined with the least squares method for threshold optimization and an error compensation model, the detection accuracy was effectively improved. Bench test results show that the detection accuracy of the device is stable above 97% at medium and low seeding frequencies of 20–40 Hz, which can meet the requirements of conventional operations. When the seeding frequency increases to 80–120 Hz, the accuracy decreases to 89.05% due to the increase in seed flow density. After introducing the compensation model, the accuracy remains above 95% in the high-frequency range of 90.2–140.2 Hz, which is nearly 10 percentage points higher than that without compensation. The research results can provide effective support and a technical approach for the accurate online detection of high-frequency seed flow in high-speed precision wheat seeding.

Keywords: high-throughput seed flow; high-speed precision seeding; photoelectric sensing detection; smart agricultural machinery; wheat

1. Introduction

China is the world's largest wheat producer in terms of both cultivated area and output. As one of China's primary staple crops, enhancing wheat yield per unit area and achieving high and stable wheat production are crucial measures for ensuring food security [1,2]. Precision seeding is the primary step in ensuring high-quality production, with the seeding rate being a critical factor within precision seeding. The seeding rate determines crop distribution density in the field and significantly impacts final crop yield. Real-time monitoring of seeding rate is fundamental to its precise control and represents an inevitable trend in smart agriculture development [3,4]. Precision wheat seeding involves high seed placement frequency, where multiple seeds pass through the detection zone simultaneously, forming a high-throughput seed stream. The interlacing and overlapping of seeds pose the primary challenge of accurate detection in such high-throughput conditions [5,6]. Under high-speed seeding conditions, the high-frequency, disordered distribution of seeds further complicates the precise detection of seed flow. Therefore, developing a real-time detection device for high-throughput wheat seed flow can enhance seeding quality, reduce

Check for updates

Academic Editor: Ray E. Sheriff

Received: 4 March 2026
Revised: 17 April 2026
Accepted: 22 April 2026
Published: 28 April 2026

Copyright: © 2026 by the authors. Licensee MDPI, Basel, Switzerland. This article is an open access article distributed under the terms and conditions of the Creative Commons Attribution (CC BY) license.

production costs, minimize seeding losses, and significantly contribute to building big data for wheat seeding operations and advancing the intelligence level of seeding [7].

Seed flow detection methods worldwide can be primarily categorized into capacitive sensing [8], piezoelectric sensing [9,10], machine vision [11], and photoelectric sensing [12]. Depending on the detection target, the detection system's adaptability and stability in complex working environments vary. Capacitive sensing systems offer strong operational stability and possess a certain degree of interference resistance in complex conditions. However, they detect only minimal capacitance changes from individual lightweight seeds, making them unsuitable for single-seed precision detection. Additionally, factors like temperature, humidity, and electromagnetic interference significantly impact the detection accuracy of capacitive sensors. Thus, detecting granular flows like wheat requires establishing relatively ideal testing environments. Piezoelectric sensors achieve precise detection at low seeding frequencies and offer cost advantages. However, they are susceptible to vibration, and high seeding frequencies cause overlapping vibration signals from multiple seeds. They also demand complex connection structures, making them unsuitable for high-frequency wheat seeding detection. Machine vision sensors are not limited by seed size and offer high detection accuracy. However, due to their high cost, stringent environmental requirements, and complex structure, they are currently largely confined to the laboratory stage and are difficult to integrate into seeders for field sowing detection.

Photoelectric seed detection systems are currently the most technically mature and widely used type of system [13–16]. Most seed monitoring systems installed on precision seeders manufactured by major international agricultural machinery companies employ photoelectric detection principles. Developed countries began exploring intelligent monitoring and control technologies for precision seeding early on and have conducted numerous experiments in this field. In 1982, Australia's A.E.E. Ltd. developed a seeding detection device that utilized infrared sensors to monitor seeds. This device employed infrared sensors mounted on the seed tubes of each row to monitor the flow of seeds within the seed tubes. If a blockage occurred, the monitor immediately activated warning lights and displayed the fault status, thereby effectively capturing seeding information during the seeding process. Karimi et al. developed an infrared sensing system based on photodiodes, capable of detecting the mass flow rate of seeds passing through the seed guide tube during the seeding process [17]. HADI et al. constructed a field seeding monitoring device and system using an infrared laser diode array sensor based on seed flow monitoring, thereby enabling the calculation of seed flow rates [18]. Rajeev et al. arranged infrared LEDs in a ring configuration to ensure that infrared light covered the entire cross-section of the seeding tube; however, this method yielded unsatisfactory detection results for small-sized seeds such as wheat [19]. Anil et al. employed an opposed-beam fiber-optic sensor for seeding flow detection, which can detect large, medium, and small-sized seeds; however, this study was limited to single-seed sowing [20].

With the continuous advancement of science and technology, intelligent monitoring and control technologies for precision seeders capable of handling crops of various particle sizes—from large to small—have gradually matured in developed countries worldwide. These machines feature a high degree of intelligence and precision in operation, and some seed-planting monitoring devices have already been commercialized. Notable examples include Sweden's Vaderstad, whose precision wheat seeder employs an optical detection system that counts passing seeds via a light-sensing array [21]. This system achieves detection frequencies up to 300 Hz with over 97% accuracy. MC Electronics of Italy has developed an infrared-based through-beam seed detection system capable of accurately detecting medium- and large-sized seeds such as wheat [22]. The system works by detecting changes in the voltage signal at the receiver when seeds block the infrared beam emitted

from the transmitter as they fall. The control system collects and processes these voltage changes to achieve precise detection of large, medium, and small-sized seeds such as wheat, soybeans, and corn. Additionally, the accompanying display unit provides real-time data on total seed output, skipped seed rate, planted area, plant spacing, and seed rate per unit area, while issuing voice alerts for blockages or malfunctions.

In China, quality inspection of intelligent precision seeders used in domestic production has primarily focused on large-seeded crops such as corn and soybeans. While monitoring and alarm systems for faults such as seed tube blockages and broken seed rows have been implemented for small- and medium-seeded crops like wheat, rice, and rapeseed, there is a lack of high-throughput seed flow detection technologies and devices, and few seeders are equipped with seed quality inspection systems. Compared to large-seeded crops, small- and medium-seeded crops have a higher seed discharge frequency (e.g., rapeseed at approximately 20–40 Hz and wheat at approximately 100–300 Hz). When inspecting small- and medium-seeded crops, the high discharge frequency of the seed sequence is irregular, making it difficult to accurately distinguish individual seeds. Additionally, challenges arise from the weak signals generated by small seeds as they pass through the sensing area and the potential for detection blind spots. These factors make it difficult to achieve precise detection of small- and medium-sized seeds. Currently, the issue of high-throughput detection of overlapping small- and medium-sized seeds remains a hot topic of research both domestically and internationally.

In response to the aforementioned challenges, Chinese researchers have actively explored the application of photoelectric detection principles in recent years for precision seed flow monitoring during the planting of small-seeded crops like wheat. Ding Youchun et al. employed a 1 mm thick thin-film laser emitter for seed flow monitoring, effectively identifying seeds with longitudinal distances exceeding 1 mm and thereby enhancing sensor resolution to some extent. However, this approach failed to fundamentally resolve the detection of overlapping seeds [23]. Ding Youchun and colleagues also attempted to divert high-throughput seed streams into four parallel detection channels. By integrating technologies such as thin-film laser-silicon photovoltaic cells, they developed a highly efficient, high-throughput detection device for small-diameter seed streams. Within the rapeseed discharge frequency range of 20.00–61.68 Hz, the detection accuracy of this device reaches a minimum of 96.1%, with the maximum detection error controlled within 3.9%; however, during high-speed sowing, when the seed discharge frequency reaches up to 130 Hz, the detection accuracy of the device decreases [24]. Recently, he has also researched and designed a solar-powered high-speed rapeseed sowing stream-splitting and synchronous detection device. This device divides the high-speed seed stream into eight low-throughput channels, incorporating an LED array light source and a silicon photodiode detection structure, with the system integrated onto an eight-channel ring-shaped surface-mount detection circuit board. Bench tests indicate that at seeding rates of 60–130 Hz, the 8-channel detection device achieves a detection accuracy of over 97.63% for rapeseed seeding rates, with the minimum detection accuracy improved by 10.03 percentage points compared to the original 4-channel detection device [25]. Xu Chunbao et al. transformed high-throughput into low-throughput multi-channel parallel synchronous detection. They proposed a method using “LED beads + narrow slits” to generate a thin light layer, combined with convex lens refraction principles to expand the effective detection area. They designed a thin-layer light refraction-based multi-channel parallel detection device for wheat seed flow. At wheat seeder operating speeds of 2–9 km/h, the detection device achieved an accuracy rate exceeding 95.28% [26]. These methods apply the principle of seed flow reconstruction to detect high seeding rates in row planting. They use a flow-splitting device to reduce seed flow density, followed by detection based on the optoelectronic principle; however, this

approach is not conducive to maintaining the original uniformity of the seed flow. Wang Zaiman et al. developed an area-source photoelectric sensor that determines seed quantity via pulse width modulation, enabling detection of rice hole numbers and seeds per hole. The average detection error range for seeds per hole was 7.99% to 24.07% [27]. Jiang Meng et al. designed a seeding rate sensor based on infrared detection principles, proposing peak and average value algorithms for determining overlapping seed counts. The developed seeding rate detection system achieved high accuracy, meeting detection requirements for seeding rates of 120–180 kg/hm^2 at operating speeds of 2.5–4.6 km/h [28]. Zhang Tian et al. designed a fiber-optic counting-based seed flow detection system for a rapeseed precision seeder using a reflective photoelectric sensing method, enabling real-time counting of the seed flow. Field trials showed that the relative deviation in rapeseed seeding rate detection did not exceed 8%, indicating that the system has a low overall error rate [29].

Practice demonstrates that photoelectric detection is a widely adopted and mature detection method with extensive application in seeding [30–32]. Photoelectric sensor-based detection devices feature low cost, non-contact sensing, and rapid signal response. However, in complex field conditions, dust accumulation on photosensitive components may reduce their responsiveness, thereby diminishing detection accuracy. Additionally, limitations in the optical layer thickness of the photosensitive area can cause signal aliasing from multiple seeds, further compromising detection precision.

In recent years, China has made some progress in the research and development of seed flow detection devices for crops such as wheat. While drawing on international design experience and incorporating innovations, certain challenges remain. For instance, there are few devices capable of single-seed precision sowing on mechanical wheat seeders and few pieces of equipment capable of maintaining stable sowing during high-speed operations. Most seed count detection devices are only capable of handling low-throughput, low-frequency detection; they exhibit significant errors during high-throughput sowing. Additionally, issues such as detection blind spots or missed counts caused by overlapping seeds remain unresolved and require urgent breakthroughs. Wheat seeds are relatively small with high seeding frequencies. During high-throughput seeding, seed overlap and interlacing may occur, causing conventional detection devices to experience double detection or missed detection. Seed flow seeding rate detection requires more precise equipment [24,33].

It should be noted that major developed countries in Europe and the United States currently use pneumatic-conveyor wheat seeders. These seeders offer advantages such as wide working widths, high operational efficiency, and fast working speeds. Through years of innovative research, foreign companies and researchers have developed comprehensive hardware and software support systems, including online monitoring systems for seeding and fertilizer application rates [34]. These countries primarily rely on large-scale farm production, whereas China's domestic fields are generally smaller. The national context of a vast country with small-scale farming operations limits the use of pneumatic-conveyance seeders. China has adopted precision wheat seeding as its primary development model, increasing wheat yields by improving traditional seeding practices and machinery. However, the performance of current seeders fails to meet the precision requirements of modern agricultural practices. Key issues include low seeding accuracy, poor uniformity, slow operating speeds, and a lack of monitoring mechanisms for seeding and fertilizer application rates, all of which limit further increases in wheat yields. In terms of precision seed metering, the market remains dominated by mechanical seed meters such as external groove wheels and dimple wheels [35]. Pneumatic seed meters are often modified from those used for corn or vegetables, resulting in a lack of precision seed meters specifically designed to match wheat planting practices [36]. Sensors for detecting wheat seeding rates

have not yet become widespread, and there is a lack of effective monitoring methods during the seeding process. Wheat seeds are small, and existing sensors have low recognition rates for them. Furthermore, since precision sowing of wheat requires a lower single-seed rate, the probability of seed overlap is high, making it difficult for sensors to accurately detect the seeding rate. Most existing detection methods are still in the laboratory research stage, and no mature products have emerged. Due to differences in detection environments and specific conditions, a "ready-made" approach is not suitable for China. Additionally, developed countries do not disclose specific technical details, and the high cost of these technologies makes their application in China quite challenging.

Therefore, this study addresses the challenges associated with high-throughput seeding in Chinese wheat seeders—specifically, the rapid descent speed of seeds and the resulting overlapping and interlacing patterns that make effective and precise detection difficult. Building upon a four-row staggered hook-tooth seed dispenser previously designed by the research team for high-throughput seeding, this study developed a corresponding seed flow detection device [37]. A dual-layer orthogonal photoelectric detection method was proposed, and bench tests were conducted to investigate the detection accuracy of the device at different dispenser rotational speeds. The aim is to provide a reference for achieving precise detection of high-throughput wheat seed flows, thereby offering technical and equipment support for stable and high wheat yields in China.

2. Materials and Methods

2.1. Structure and Working Principle of the Detection Device

In this study, a four-layer staggered hook-tooth seed metering device developed previously by the research group was used as the carrier. This metering device achieves single-seed filling by means of hook-tooth holes. The staggered arrangement of hook teeth forms an interlaced and orderly seed surface in the falling seed flow, reduces collision and overlapping among seeds, and effectively improves seed orderliness. Its working principle is shown in Figure 1.

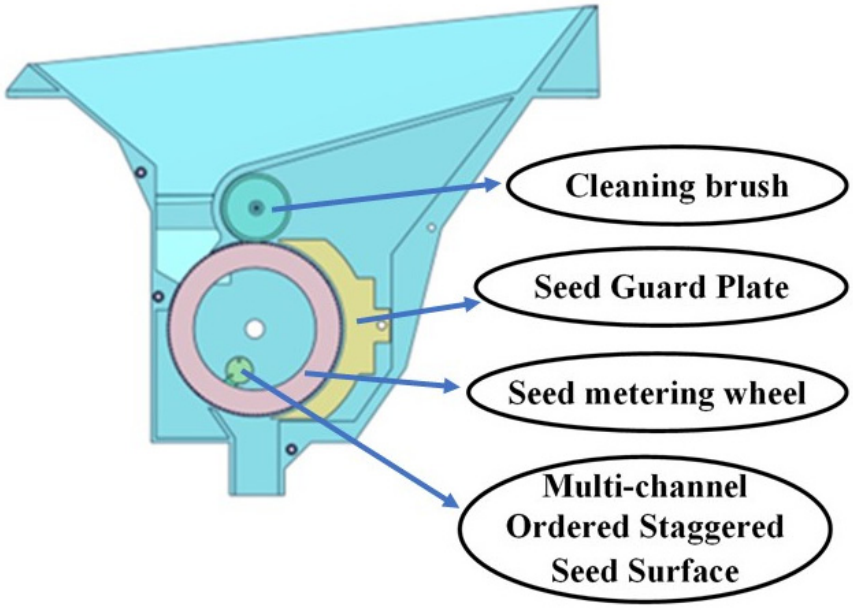


Figure 1. Structure and working principle of the seed dispenser.

The four-layer interlocking-tooth precision seed dispenser originally designed by the research team can inherently reduce seed drop density per unit time to some extent, forming a seed stream with defined time intervals. However, under high-throughput

seeding conditions, the large volume of seeds falling within a concentrated timeframe can cause seeds passing through the sensor in rapid succession to form a curtain-like obstruction effect. Furthermore, during the process of entering the seed guide tube and detection device, seeds still exhibit a certain degree of overlap and interlacing, affecting detection accuracy and even making detection difficult.

This study designed an orthogonal dual-layer photoelectric sensing detection device that performs two-stage detection on different planes of the same seed stream using two sets of sensors, thereby enabling effective identification of overlapping seeds. The detection device consists of three parts: an upper tube port, a detection zone, and a lower tube port, all of which are secured via snap-fit connectors. The upper tube port interfaces with the seed feeder of the seeder, while the two sets of sensors are embedded in the upper and lower mounting slots of the detection zone, respectively. This configuration forms a dual-layer, orthogonal detection optical path, allowing seeds to pass through the detection zone smoothly and without collision, thereby enabling the collection of signals from both surfaces. The detection device employs a BG-AG15N through-beam multi-beam infrared photoelectric sensor, which is manufactured by Shenzhen Boyi Jingke Technology Co., Ltd., Shenzhen City, Guangdong Province, People's Republic of China. This sensor consists of a transmitter and a receiver; the transmitter integrates multiple parallel infrared emitter tubes, while the receiver corresponds to independent receiver tubes. The spacing between individual beams is 1.5 mm, and the effective detection distance between the transmitter and receiver is 40 mm, making it suitable for through-beam detection of small-diameter seeds. It employs an NPN open-collector output with amplification, cutoff, and saturation operating modes [38]. A low-level signal is output when a seed passes through the optical path to trigger the sensor; the circuit is open when there is no obstruction, enabling precise detection of seed drop events. It operates on 10–30 VDC, features built-in short-circuit protection, and is equipped with three-color status indicator lights (power/operation/fault). With a response time of <1 ms, it meets the real-time data acquisition requirements of high-throughput seed dispensing scenarios. The overall structure of the detection device and a physical model are shown in Figure 2, while the overall dimensions and performance parameters are listed in Table 1.

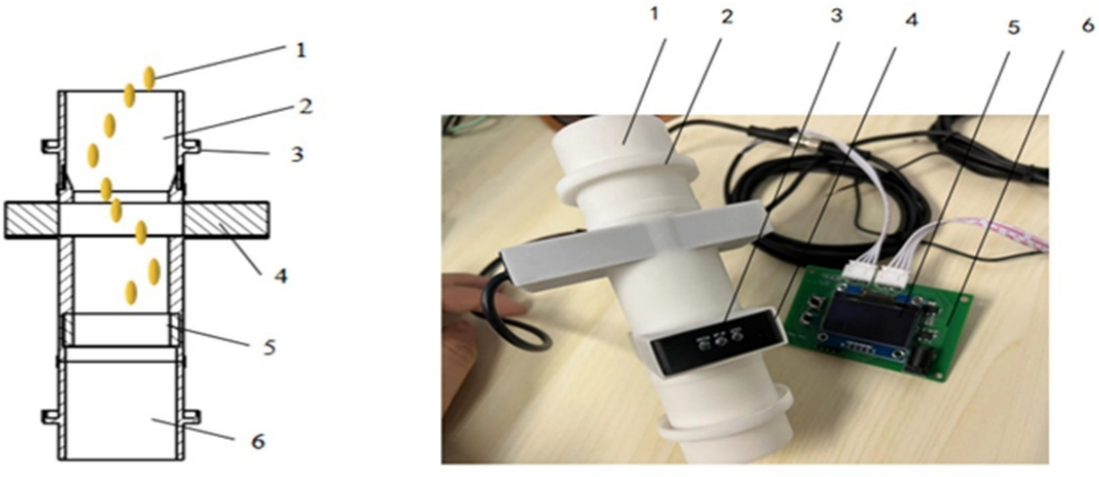


Figure 2. (**a**) Cross-sectional view of the overall structure of the detection device. (**b**) Photograph of the actual device.

Table 1. Overall dimensions and performance parameters.

Category	Specific Parameters
Length × Width × Height/mm × mm × mm	150 × 40 × 40
Pipe Diameter/mm	36
Working Hours/h	8
Time resolution/ms	1

The detection device operates as follows: As seed streams traverse the detection zone, varying seed orientations and quantities cause seeds to block light when passing through the first sensor layer, triggering corresponding electrical signal changes. As seeds continue falling through the second sensor layer—arranged orthogonally to the first—they are detected from another angle, generating corresponding voltage signals. Both signals are stored in the microcontroller. By comparing and analyzing these signals against predefined characteristics for single-seed, multi-seed, and different seed orientation patterns as they pass through the sensors, the system ultimately calculates the number of seeds passing per unit time, achieving precise counting of wheat seed streams. Additionally, to minimize errors caused by repeated detection of the same seed by different sensors due to seed length, a specific interval is maintained between the two sensor sets.

2.2. Design of Key Structural Parameters for Detection Devices

The detection device connects to the seed guide tube of the seed dispenser. Its upper tube opening has an outer diameter of 40 mm and an inner diameter of 36 mm, matching the dimensions of the guide tube for seamless connection. The upper inner surface of the intermediate seat features a conical convergence structure with an inner cone height of 8 mm. The cone surface forms a 72.68° angle with the upper pipe opening end face, guiding falling seeds to minimize collision and bounce effects on detection accuracy. The sensor's effective detection area is a 31 mm × 40 mm rectangle, with both transmitter and receiver faces measuring 31 mm in length. Through a dual-layer orthogonal arrangement, the upper and lower layers form an equivalent square detection surface of 31 mm × 31 mm, enhancing detection coverage and stability.

Based on the application scenario of the seed dispenser designed in this paper, our research group selected Ningmai No. 9 seeds—commonly used in the middle and lower reaches of the Yangtze River—as the study subject. A random sample of 300 seeds was taken, and their length, width, and thickness were measured using a vernier caliper (accuracy 0.01 mm). The measurement results yielded the three-axis dimensions of Ningmai No. 9 seeds as 6.32 mm × 3.29 mm × 2.71 mm. Given the seed's maximum length of 6.32 mm, overlapping during descent is possible. To ensure seeds are not detected by both sensors simultaneously and to account for sensor response time, the sensor spacing was set to 30 mm. This spacing guarantees the detection of seeds in identical descent postures across different time intervals within the sensors' response time. The optical layer thickness at the emitter end is 2 mm, and each sensor has a response time of 1 ms. Therefore, the seed fall process must be analyzed to verify whether the transit time meets requirements. To understand seed fall behavior, EDEM software Version 24 was used to simulate the state of seeds passing through the sensor monitoring area [39].

The simulation parameters are described below. The wheat seed is modeled as an ellipsoid, simplified to a major axis of a = 6.32 mm and a minor axis of b = 3.00 mm. Since wheat seeds have a smooth surface and no adhesion, a non-slip contact model is selected. The discrete element model (DEM) for the wheat grains was constructed using a combination of five spheres. During the simulation, wheat seed dimensions are generated according to a normal distribution. Based on available data, the material properties of the

wheat seeds and the seeding wheel, as well as their interaction parameters, are determined as shown in Table 2.

Table 2. Simulation parameter table.

Simulation Parameters	Value
Poisson's ratio of wheat seeds	0.25
Poisson's ratio of resin material	0.40
Shear modulus of wheat/MPa	1.1×10^7
Shear modulus of resin material/MPa	1.6×10^8
Density of wheat/kg·m^{-3}	1350
Density of resin material/kg·m^{-3}	1117
Coefficient of static friction between wheat and wheat	0.5
Coefficient of kinetic friction between wheat and wheat	0.5
Coefficient of recovery between wheat and wheat	0.5
Coefficient of static friction between wheat and resin	0.4
Coefficient of kinetic friction between wheat and resin	0.4
Coefficient of recovery between wheat and resin	0.45

The simulation setup involved seeds flowing from a four-layer interlocking gear feeder, with 1000 seeds and a simulation duration of 10 s. The initial velocity of seeds entering the detection zone was calculated based on the maximum seeding speed, yielding a value of 0.154 m/s. Since seeds possess initial velocity upon exiting the feeder, they undergo accelerated motion within the detection zone, as described by Equation (1).

$$\begin{cases} h_1 = \left(v_0 t_1 + \frac{1}{2} g t_1^2\right) \\ h_2 = \left(v_1 t_2 + \frac{1}{2} g t_2^2\right) \\ v_0 = rw \\ v_1 = v_0 + g t_1 \end{cases} \quad (1)$$

In the equation, h_1 is the distance from seed tube outlet to first sensor, m; h_2 is the distance between the detection surfaces of the first and second sensors, m; v_0 is the initial velocity, m/s; t_1 is the time from seed exit of seed tube to first sensor, s; v_1 is the seed velocity within the detection zone, m/s; and t_2 is the time to traverse the detection zone, s.

To verify whether the sensor response time meets detection requirements, a kinematic analysis of the seed descent process was conducted. The distance from the seed outlet to the first detector's sensing plane is known to be 50 mm, and the spacing between the two sensor sensing planes is 30 mm. Calculations show the time from seed exit to the first sensor is 0.086 s, and the time traversing both detection surfaces is 0.027 s, resulting in a total traversal time of approximately 113 ms. This duration significantly exceeds the sensor's 1 ms response time, ensuring seeds are detected within the sensor's response window and meeting detection requirements.

2.3. Signal Processing Circuit Design

To analyze and process wheat seed collection signals, an orthogonal dual-layer signal acquisition system circuit was designed. This circuit primarily consists of a power conversion circuit, a signal processing module circuit, and a display module circuit. During operation, sensors detect partial obstructions caused by wheat seeds of varying quantities and orientations crossing the sensing plane, generating distinct signals. After optocoupler isolation, these signals are input to separate interrupt pins of the microcontroller. The microcontroller processes and compares the signals before transmitting them to the display

module. Real-time results are shown on the OLED screen. The overall system circuit is illustrated in Figure 3.

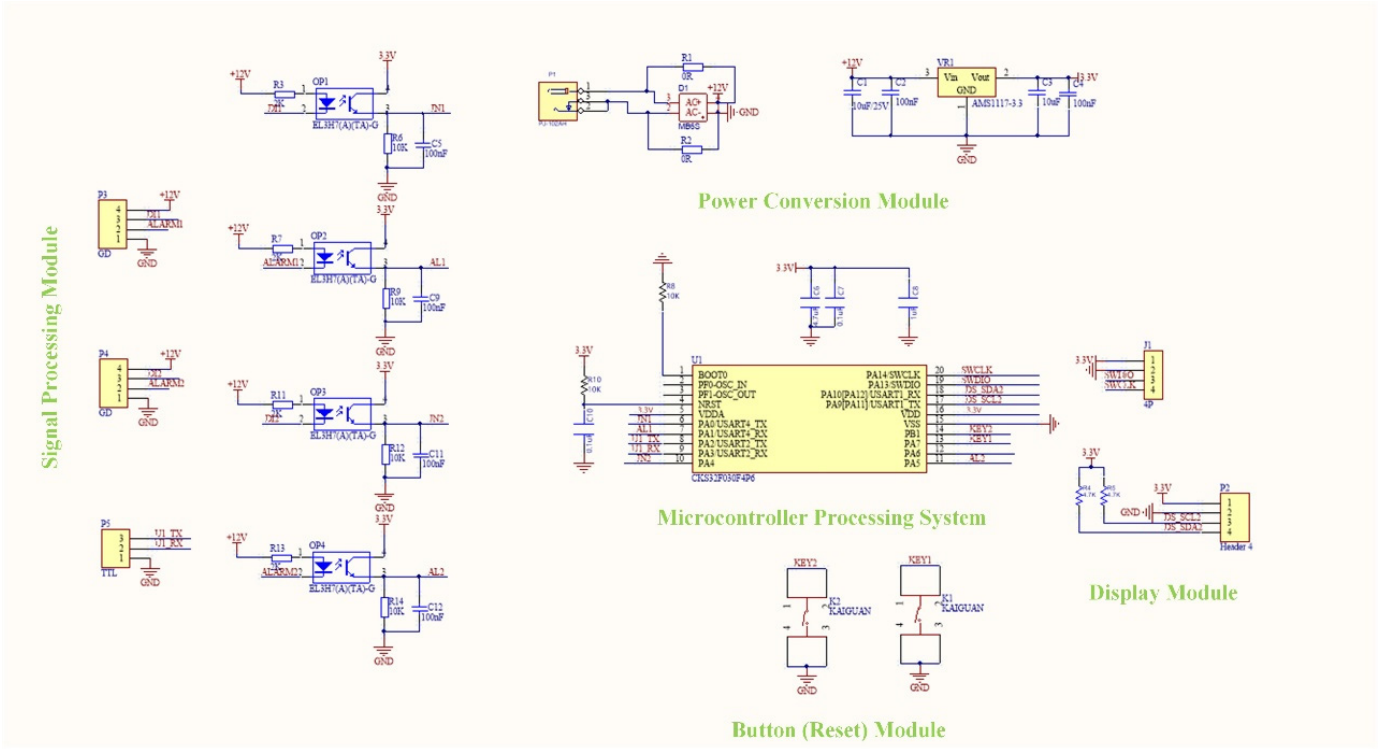


Figure 3. Overall circuit diagram of the signal processing system.

The power module utilizes a 12 V external lithium battery connected to the circuit board via a power interface. The sensor features an NPN output type, requiring its signal line to share ground with the negative terminal. As the circuit board incorporates an internal power supply, the 12 V lithium battery is connected in reverse polarity. This input is converted to +3.3 V through a power conversion circuit, providing stable power to all board components. In the signal processing and display module, optocouplers utilize light as a medium for signal coupling transmission. They offer advantages such as compact size, long lifespan, contactless operation, and strong anti-interference capabilities. They enable electrical isolation between input and output while ensuring unidirectional signal transmission, thereby stabilizing microcontroller input signals to enhance processing accuracy [40]. This design adopts the EL3H7(A)(TA)-G optocoupler manufactured by Everlight Electronics Co., Ltd., Taipei, Taiwan, China, which is capable of processing signals from two sensors. The display module employs a 1.3-inch four-pin OLED screen. Pins 1–4 connect to the microcontroller's 3.3 V, GND, DS SCL2, and DS SDA2 pins, respectively, providing a real-time display of detected seed flow counts. The reset button module clears test data and switches display interfaces. After each signal processing cycle, the recorded data is displayed. A new test cycle requires resetting via this module to restart counting. Since both sensors can operate independently, three display interfaces are configured: upper sensor detection data, lower sensor detection data, and upper–lower comparison detection data.

2.4. Program Design

The signal processing system program for the orthogonal dual-layer sensor is crucial for achieving seed flow detection and counting. Designed to enable precise detection of wheat seed flow, this software program first completes zero-point calibration, system

initialization, interrupt initialization, and OLED display initialization upon startup before entering a continuous detection state. The system employs dual-layer interleaved sensors for detection, utilizing isolated input circuits to ensure independent operation and mutual interference-free functioning of both sensor channels. As seeds sequentially pass through both sensors, their output signals are separately acquired and stored. Within a unit time interval, the two signals are compared and evaluated. If the counts match, the result is directly displayed. If they differ, the higher value is selected as the final count. Should the difference between the two detection values exceed 4, the alarm light flashes and detection pauses. The final count result is displayed in real time via the OLED screen. The wheat seed flow counting program is illustrated in Figure 4.

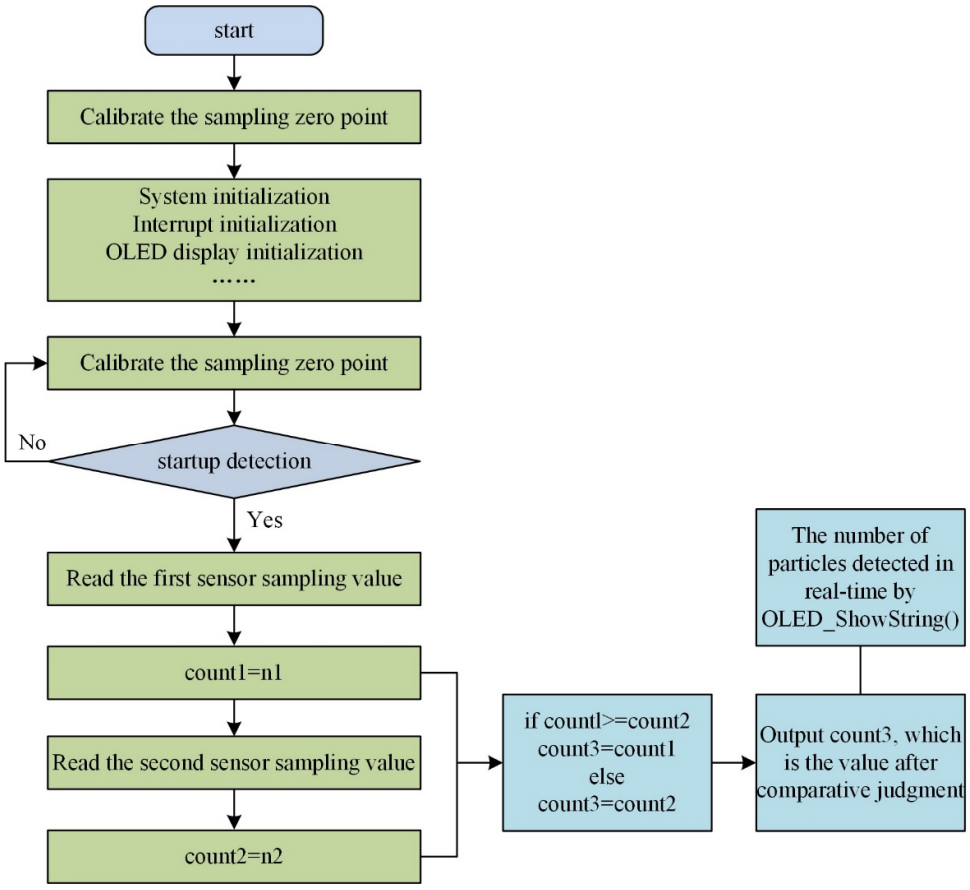


Figure 4. Flowchart for wheat seed counting program.

2.5. Signal Propagation Analysis

Based on preliminary test results and agronomic requirements, the wheat seed rate is 15 kg per mu. The selected Ningmai 9 variety has a thousand-grain weight of 40.1 g, and the specified travel speed must reach 6–8 km/h. During the same time interval, no more than four seeds pass through the sensor, with most passing the detection surface in pairs. Accordingly, this detection device prioritizes enhancing recognition accuracy and counting stability for 1–4 seeds.

To verify whether the sensor exhibits missed detection or blind spots, a low-frequency single-seed drop test was conducted on the assembled detection device. Well-formed, undamaged wheat seeds were selected for testing. Single-seed tests were performed at varying drop heights and orientations, with all 200 seeds effectively detected. Counting results were recorded in real time via the display screen to determine whether each seed was correctly identified. Test results confirmed no missed detections under low-frequency single-seed

testing conditions, validating the rationality of the device's structural design and detection reliability. The low-frequency single-seed detection test is illustrated in Figure 5.

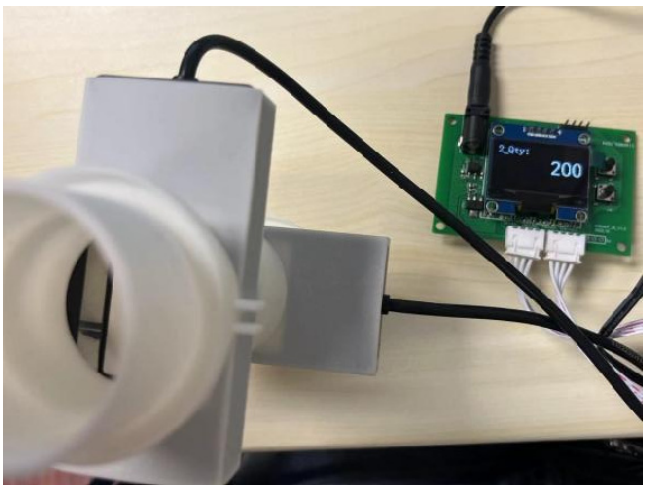


Figure 5. Low-frequency single-particle detection device.

To investigate how the sensor detects seeds of varying quantities and orientations, experimental analysis was conducted on the signal changes caused by the fall of 1, 2, 3, and 4 seeds. The experiment involved collecting voltage signal values altered by the fall of single to four seeds through the detection device. The test was divided into four groups, each comprising falls of 1 to 4 seeds. Since seeds assume different orientations during fall, resulting in varying signals, a single sensor array was used for testing. Each group of tests was repeated 100 times.

2.6. Bench Testing

This study used Ningmai 9 wheat seeds as the experimental material. Before the experiment, damaged and shriveled seeds were manually removed. The research was conducted using a four-layer interlocking-tooth wheat seed dispenser developed by the research team and a seed flow detection apparatus test rig, as shown in Figure 6.

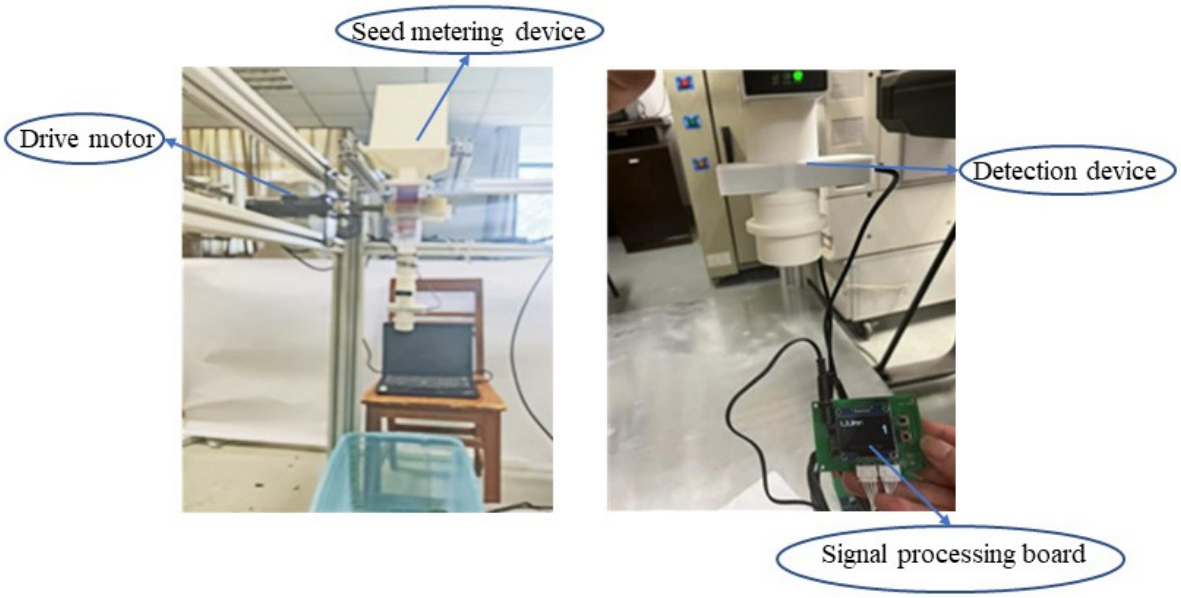


Figure 6. Test bench site photo.

To investigate whether the performance of the designed detection device meets the seeding frequency of the seed dispenser, bench tests were conducted on the wheat seed flow detection device at different frequencies using the constructed test rig to evaluate its performance. Combined tests were performed with the detection device and seed dispenser to verify the detection accuracy at various rotational speeds of the seed dispenser.

The specific bench test methodology is as follows:

(1) Before testing, intact wheat seeds without damage were selected to prevent detection errors caused by seed defects. An automatic seed counter simulated the seeder's operation, setting two tiers of sowing frequencies: low frequency (20 Hz, 25 Hz, 30 Hz) and high frequency (80 Hz, 100 Hz, 120 Hz). The sowing rate was 15 kg, with an operating speed of 6–8 km/h. Each seeding cycle lasted 10 s, and each frequency setting was repeated three times.

(2) Connect the detection device to the seed distributor to evaluate detection accuracy at different distributor wheel speeds. Set the seed distributor to a uniform seed layer height of 65 mm. Test five distributor wheel speed settings: 14 rpm, 16 rpm, 18 rpm, 20 rpm, and 22 rpm. Seed for 10 s at each speed, repeating each speed setting three times.

(3) Collect seeds dispensed at different frequencies and seeder speeds into pre-labeled bags. After testing, verify the actual number of seeds dispensed.

3. Results and Discussion

3.1. Signal Propagation Analysis Results

Sampling values for 1 to 4 seeds may exhibit overlapping intervals, requiring experimental determination of the judgment range for different seed counts. All experiments were conducted in a clean indoor bench setup, and the wheat seeds were carefully screened to ensure high purity, so no noise caused by dust, chaff, or debris appeared in the sampling signals. The sensor's output voltage is correlated with the seed occlusion area; consequently, more seeds passing through the detection zone simultaneously produce a stronger response and higher sampling peak. The maximum sampling peak observed across all tests was 500, with no values exceeding this limit, and no data scrubbing was performed. By recording and analyzing peak values from multiple repeated tests, the classification thresholds were determined. The distribution of sensor detection peaks is presented in Figure 7.

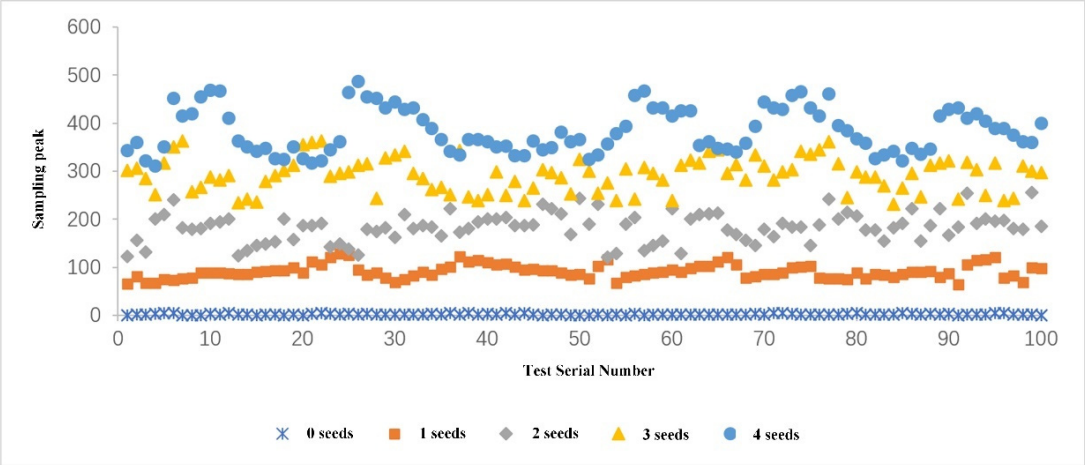


Figure 7. Peak distribution detected by sensors.

As shown in Figure 7, when no seeds pass through the detection device, the voltage detection peak is 0, indicating that the detection system is unaffected by external factors

and exhibits stable performance. When 1 seed and 2 seeds pass through, the overlapping peak sampling interval is [65, 128]; when 2 seeds and 3 seeds pass through, the overlapping interval is [122, 256]; and when 3 and 4 seeds pass, the overlap interval is [234, 362].

Preliminary tests have shown that as the number of seeds in the detection area increases, the sensor voltage rises; that is, the voltage sampling peak (the maximum value among multiple samples, expressed as a numerical value) becomes larger. The sampling peaks for different seed counts are classified using the binary search method. When the theoretical detection error is minimized, this peak is set as the discrimination threshold for different seed counts. To determine the classification threshold, the theoretical detection error η is introduced as the threshold evaluation metric [41]. Calculations yield the following discrimination values: 85 for distinguishing 1 seed from 2 seeds, 168 for 2 seeds vs. 3 seeds, and 314 for 3 seeds vs. 4 seeds. Thus, values 0–85 are classified as 1 seed, 85–168 as 2 seeds, 168–304 as 3 seeds, and >304 as 4 seeds. Therefore, the total theoretical detection error is 5.74%.

The theoretical detection error is calculated as follows:

$$\begin{cases} \eta_1 = \frac{n_1\lambda+2n_2\tau}{300} \times 100\% \\ \eta_2 = \frac{2n_3\tau+3n_4\varphi}{500} \times 100\% \\ \eta_3 = \frac{3n_5\varphi+4n_6\rho}{700} \times 100\% \\ \eta = \eta_1 + \eta_2 + \eta_3 \end{cases} \quad (2)$$

In the formula, n_1 is one grain mistakenly counted as two grains; n_2 is 2 grains miscounted as 1 grain; n_3 is 2 grains mistakenly counted as 3 grains; n_4 is 3 grains mistakenly counted as 2 grains; n_5 is 3 grains mistakenly counted as 4 grains; n_6 is 4 grains mistakenly counted as 3 grains; λ, τ, ϕ, ρ represent the probability that 1, 2, 3, or 4 seeds pass through the detection zone, %; and η_1, η_2, η_3 represent the theoretical detection error between different particle counts.

3.2. Analysis of Bench Test Results

3.2.1. The Influence of Seeding Frequency on Detection Results

After completing the bench test, the experimental results within the seeding frequencies of 20–30 Hz and 80–120 Hz are shown in Table 3, while those within the seeding wheel speeds of 14–22 r/min are presented in Table 4.

Table 3. Test results of the detection device under different seeding frequencies.

Seeding Frequency/Hz	Seeding Time/s	Total Number of Detections/Grain	Actual Total Number/Grain	Detection Accuracy/%
20	10	202	205	98.54 ± 0.23
20	10	298	201	98.51 ± 0.31
20	10	198	200	99.00 ± 0.27
30	10	294	302	97.35 ± 0.35
30	10	298	304	98.03 ± 0.29
30	10	299	308	97.08 ± 0.32
40	10	393	402	97.76 ± 0.25
40	10	399	408	97.79 ± 0.28
40	10	398	405	98.27 ± 0.26
80	10	781	810	96.48 ± 0.34
80	10	778	808	96.29 ± 0.38
80	10	769	802	95.88 ± 0.41
100	10	932	1001	93.11 ± 0.45
100	10	929	1008	92.16 ± 0.49
100	10	936	1006	93.04 ± 0.43
120	10	1074	1206	89.05 ± 0.52
120	10	1076	1202	89.52 ± 0.50
120	10	1081	1200	90.08 ± 0.47

Table 4. Test results of the performance of the detection device at different rotational speeds.

Seed Metering Wheel Speed/r/min	Seeding Time/s	Seeding Frequency	Total Number of Detections/Grain	Actual Total Number/Grain	Detection Accuracy/%
14	10	86.4	828	864	95.83 ± 0.26
14	10	86.8	834	868	96.08 ± 0.24
14	10	87.2	842	872	96.56 ± 0.22
16	10	96.2	914	962	95.01 ± 0.29
16	10	97.1	911	971	93.82 ± 0.33
16	10	95.8	903	958	94.26 ± 0.31
18	10	117.4	1057	1174	93.03 ± 0.36
18	10	118.2	1065	1182	90.10 ± 0.42
18	10	117.8	1070	1178	90.83 ± 0.40
20	10	127.6	1135	1276	88.95 ± 0.45
20	10	125.8	1123	1258	89.27 ± 0.44
20	10	126.6	1126	1266	88.94 ± 0.46
22	10	139.2	1209	1392	86.85 ± 0.51
22	10	138.2	1203	1382	87.05 ± 0.50
22	10	137.9	1210	1379	87.74 ± 0.48

Bench test results (Table 3) indicate that the detection performance of the dual-layer orthogonal photoelectric wheat seed flow detection device exhibits a significant variation pattern with seed discharge frequency. At low to medium seed discharge frequencies (20–40 Hz), the device's detection accuracy remained stable at over 97%, with some test groups reaching over 98% and a maximum of 99.00 ± 0.27%; simultaneously, the standard deviation in this range was generally less than 0.35%, with extremely low dispersion and excellent repeatability of the detection results. This indicates that the device possesses outstanding reliability and stability under low-to-medium-throughput seed flow detection conditions and can meet the precise counting requirements of routine seeding operations.

When the seeding frequency was increased to the high-throughput range of 80–120 Hz, the detection accuracy showed a significant decline, and the standard deviation continued to increase with rising frequency, while detection stability simultaneously decreased: at 80 Hz, the accuracy remained between 95.88% and 96.48%, with a standard deviation of 0.34–0.41%, representing a slight decline compared to the medium-to-low frequency range, and an increase in the fluctuation of detection results; at 100 Hz, the accuracy rate dropped to 92.16–93.11%, and the standard deviation rose to 0.43–0.49%; and at 120 Hz, it further decreased to 89.05–90.08%, falling below 90%, with a standard deviation of 0.47–0.52%. This trend indicates that as seed flow density and throughput speed increase, the probability of seed overlap and signal crosstalk rises significantly, placing greater demands on sensor signal processing and recognition. Consequently, the probability of missed or false detections increases, leading not only to a significant decrease in detection accuracy as seeding frequency rises but also to a marked deterioration in the stability and repeatability of detection results.

Overall, this dual-layer orthogonal photoelectric detection device demonstrates excellent performance with high accuracy and stability at low to medium seeding frequencies (20–40 Hz), capable of meeting the precise counting requirements of routine seeding operations. Meanwhile, the patterns of accuracy and stability degradation observed in high-throughput scenarios provide clear directions for optimizing the device's operational conditions and for future upgrades (such as compensation for overlapping seeds).

Regarding the impact of seed wheel rotational speed, as the speed increased from 14 r/min to 22 r/min, detection accuracy steadily declined from a peak of 96.56 ± 0.22% to 86.85 ± 0.51%, with the standard deviation of detection results showing a synchronous upward trend, which fully reflects the change in detection stability with rotational speed.

Within the low-to-medium speed range of 14–16 r/min, the device demonstrated stable and reliable performance, maintaining an accuracy rate above 93% (with the highest accuracy reaching 96.56 ± 0.22%). Meanwhile, the standard deviation in this speed range was generally below 0.33%, indicating extremely low data dispersion and excellent repeatability of detection results, verifying that the device can meet the accurate counting requirements of conventional seeding operations under low-to-medium speed conditions.

However, accuracy declined significantly when the speed exceeded 18 r/min, falling below 90% at 20 r/min and above, and the standard deviation increased synchronously: at 18 r/min, the standard deviation rose to 0.36–0.42%; at 20 r/min, it further increased to 0.44–0.46%; and at 22 r/min, the standard deviation reached 0.48–0.51%. This variation is highly correlated with the operational characteristics of the seed dispenser: as the seed wheel speed increases, the seeding frequency rises, leading to higher seed flow density and accelerated passage speed. This increases the probability of seed overlap and collision on the detection surface while simultaneously reducing the seed qualification rate. Consequently, the detection device faces greater recognition challenges, ultimately manifesting as a decrease in detection accuracy and a deterioration in detection stability with increasing rotational speed.

Overall, the detection device delivers outstanding performance under medium-to-low throughput and medium-to-low seed metering wheel speeds, with high detection accuracy and excellent stability that fully meet the design requirements for Chinese wheat precision seeders. Although the detection accuracy and stability deteriorate under high-throughput and high-speed seeding conditions due to increased seed overlap and signal interference, the device still maintains a certain level of effective detection capability, providing a practical technical solution for conventional seeding operations and a clear direction for further performance optimization.

3.2.2. Establishment of the Compensation Model and Analysis of Test Results

Since the detection device's accuracy failed to meet the specified range, an error compensation model was established to enhance seed metering accuracy. The device underwent accuracy verification testing after implementing the compensation model.

First, the data from Tables 2 and 3 were consolidated and subjected to further processing and analysis. Since the seeder's seeding frequency exceeded 80 Hz, only data above 80 Hz was analyzed. The relationship curve between detection accuracy and seed metering frequency was fitted using Excel, and the fitted variation curve is shown in Figure 8.

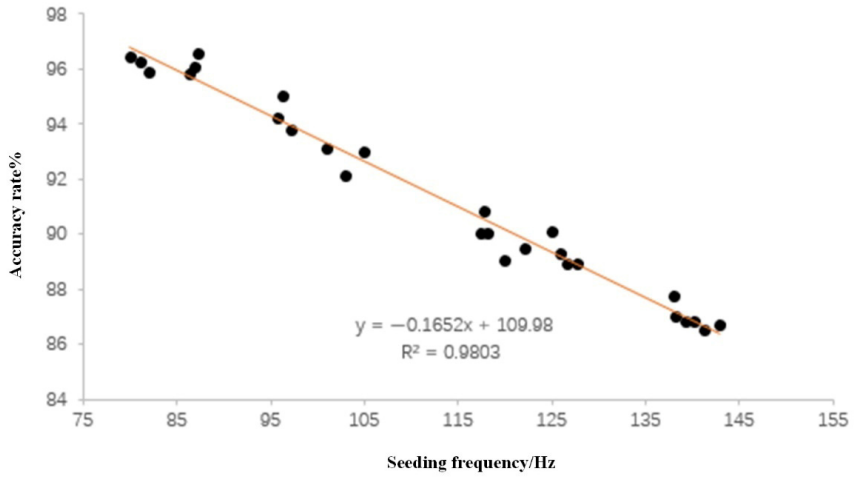


Figure 8. Curve showing the relationship between the seeding frequency of wheat seeds and the change in detection accuracy.

It can be concluded from Figure 8 that the detection accuracy of the detection device decreases as the seeding frequency gradually increases, and the linear trend of accuracy becomes lower later on. In the fitting curve, the linear correlation between seeding frequency and detection accuracy is 0.9803, indicating a high data consistency. The fitted linear equation is as follows:

$$f(x) = -0.1652x + 109.98 \ (x > 80) \tag{3}$$

To further improve the detection accuracy and make it closer to the actual sowing rate, a compensation model was established based on the curve fitted from previous test data.

The fitting curve formula is as follows:

$$y = 1.3834x - 29.097 \ (R^2 = 0.9989) \tag{4}$$

The formula for the compensation model is as follows:

$$I' = KI \tag{5}$$

In the formula: I' is the number of grains detected after compensation, grain; K is the compensation coefficient value of 1.3834; and I is the number of grains detected before compensation, in grains.

Upon the construction of the seed quantity compensation model, the detection precision of the wheat seed flow monitoring system was significantly enhanced. To verify the detection accuracy after compensation, bench tests were carried out under different seeding speeds. With the same seed-filling layer height of 65 mm, seeding was performed at different rotational speeds for 10 s. The test results are shown in Table 4, and the scatter plot of the results is shown in Figure 9.

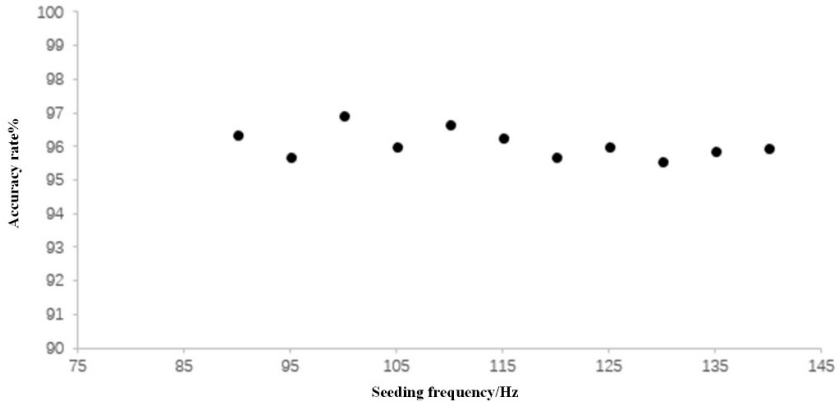


Figure 9. Distribution map of results after using the compensation model in the wheat seed flow detection device.

By comparing the detection results before and after the establishment of the compensation model, it can be seen that within the seeding frequency range of 90.2–140.2 Hz, the detection accuracy after establishing the compensation model remains stable above 95%. Compared with the working conditions of the same frequency without using the compensation model, the accuracy is improved by nearly 10 percentage points at most, which significantly improves the detection performance under high-frequency seeding and effectively enhances the detection accuracy and reliability of the device in high-throughput seed flow scenarios.

4. Conclusions

Based on an analysis of the current status and development trends of wheat seed flow detection technology at home and abroad, this paper carries out innovative design and experimental research on a high-throughput wheat seed flow detection device. Currently, foreign advanced systems focus on large-scale precision seeding with high detection accuracy, but they are expensive, poorly compatible with domestic planters, and their technical details are not publicly disclosed. Domestically, there are few breakthroughs in high-throughput overlapping detection for small-grain seeds, and the main research trends focus on high-throughput adaptability, anti-interference ability, and compatibility with local agricultural machinery. Future research on high-throughput seed flow overlapping detection can focus on high-speed precision detection, universal detection of multiple seed varieties, establishment of detection standards, integration of cutting-edge technologies, and in-depth mining of detection information. In particular, for high-speed precision detection, efforts can be made to further tackle the ordered shunting and seeding of high-throughput seed flow and surface source detection technology based on multi-channel light beams, so as to solve the problem of missing records caused by overlapping high-throughput seed flow or passing through detection blind areas and improve detection accuracy.

Relying on the four-layer interleaved hook-tooth seed metering device independently developed by the research team, this study designed an orthogonal double-layer photoelectric wheat seed flow detection device. This device can effectively identify interleaved and overlapping wheat seeds and realize stable detection of the high-throughput seed descent process. This study completed the structural design of the detection device, built a signal detection system, and verified it through bench tests. The main conclusions are as follows:

(1) A dual-layer orthogonal photoelectric wheat seed flow detection device was developed, capable of reliable docking with the seed feeder's seed guide tube to enable real-time monitoring of seeding rates. By optimizing the housing structure, seeds enter the detection zone smoothly without collision, ensuring uninterrupted seed delivery. This effectively addresses challenges in high-throughput seeding, such as large seed volumes, high frequency, and seed overlap. The dual-layer orthogonal photodetectors capture seeds falling simultaneously at different planes. Seed quantity is determined by voltage changes caused by light blockage at each plane, with dual-plane signal comparison enhancing counting accuracy.

(2) A dual-layer orthogonal photoelectric wheat seed flow signal detection system was established. To address signal overlap in multi-seed sampling, signal penetration characteristics were analyzed to identify voltage peak distribution patterns for different seed counts. Using least squares optimization, differentiation thresholds for adjacent seed counts were derived, and a multi-seed misjudgment error calculation model was established, effectively resolving misjudgments caused by signal overlap.

(3) Bench test results indicate that the detection device's performance is influenced by seeding frequency. At medium–low frequencies (20–40 Hz), detection accuracy remains stable above 97%, meeting conventional seeding requirements. When the seeding frequency increases to 80–120 Hz, the detection accuracy drops to 89.05% due to increased seed flow density. After introducing the compensation model, detection accuracy remained stable above 95% within the high-frequency range of 90.2–140.2 Hz. This represents a maximum improvement of nearly 10 percentage points compared to the uncompensated state, significantly enhancing detection reliability under high-frequency conditions.

Author Contributions: Conceptualization: H.Z., B.Q., Y.W. and S.H.; Methodology: H.Z., B.Q., Y.W. and S.H.; Software: H.Z., Y.D. and S.H.; Validation: H.Z., B.Q. and Y.W.; Formal Analysis: H.Z., B.Q. and Y.W.; Investigation: H.Z., B.Q. and Y.W.; Resources: B.Q.; Data Curation: H.Z. and S.H.;

Writing—Original Draft Preparation: H.Z. and S.H.; Writing—Review and Editing: H.Z., B.Q. and Y.W.; Visualization: H.Z. and B.Q.; Supervision: B.Q. and Y.W.; Project Administration: B.Q., Y.W. and W.Z.; Funding Acquisition: B.Q., Y.W. and Y.D. All authors have read and agreed to the published version of the manuscript.

Funding: This research was funded by the National Key Research and Development Program of China (2021YFD2000402); the Science and Technology Innovation Program of the Chinese Academy of Agricultural Sciences (CAAS-SAE-202301); the Jiangsu Modern Agricultural Machinery Equipment and Technology Promotion Project (NJ2025-03); and the Jiangsu Provincial Key Technology Integration and Promotion Project for Modern Agriculture: JCTG [2025]06-7.

Institutional Review Board Statement: Not applicable.

Informed Consent Statement: Not applicable.

Data Availability Statement: The original contributions presented in this study are included in the article. Further inquiries can be directed to the corresponding authors.

Acknowledgments: We would like to thank all the co-authors and the reviewers, whose valuable feedback, suggestions and comments significantly increased the overall quality of this review.

Conflicts of Interest: Authors declare that the research was conducted in the absence of any commercial or financial relationships that could be construed as potential conflicts of interest.

References

1. National Bureau of Statistics' Announcement on Grain Output Data for 2025. Available online: https://www.stats.gov.cn/sj/zxfb/202512/t20251212_1962049.html (accessed on 3 March 2026).
2. Wang, H.; Zhang, C.P.; Peng, H.; Xu, W.H. Current Situation, Existing Problems and Policy Suggestions of China's Wheat Industry. *Grain Issues Res.* **2025**, 4–9. Available online: https://kns.cnki.net/KCMS/detail/detail.aspx?dbcode=CJFQ&dbname=CJFDLAST2026&filename=LSWY202506001 (accessed on 3 March 2026).
3. Liao, Y.T.; Tan, Y.; Liao, Q.X.; Zheng, J.; Wang, L.S.; Zhang, Q.S. Research Progress and Development Trends in Precision Seeding Technologies for Major Grain and Oil Crops. *Trans. Chin. Soc. Agric. Mach.* **2025**, *56*, 1–19.
4. Wang, X.; Zhang, K.L.; Zhang, D.X.; Mu, J.S.; Yin, X.W.; Cui, T.; He, X.T.; Yang, L. Research Progress on Unmanned Precision Seeding Technology and Equipment for Major Grain and Oil Crops. *Trans. Chin. Soc. Agric. Mach.* **2025**, *56*, 21–41.
5. Wang, Y.; Song, C.; Gao, Y.; Lan, Y.; Wang, G.; Ming, R. Mass Flow Detection Technology for Seed and Fertiliser Particles and Its Application in Uav-Based Spreading. *Inmateh-Agric. Eng.* **2025**, *75*, 584–599. [CrossRef]
6. Liu, W. Research on Seeding Rate Monitoring and Controlling Technology Based on Information of Seed Flow Rate for Wheat Drill. Doctoral Dissertation, Jiangsu University, Zhenjiang, China, 2022.
7. Guan, X.; Nie, S.; Ge, H.; Ding, Y.; Yang, J. Research Status and Development Trends of Adjustable Precision Seeders. *Agronomy* **2026**, *16*, 495. [CrossRef]
8. Zhou, L.M.; Zhang, X.C.; Yuan, Y.W. Design of capacitance seed rate sensor of wheat planter. *Trans. Chin. Soc. Agric. Eng.* **2010**, *26*, 99–103. [CrossRef]
9. Ding, Y.C.; Yang, J.Q.; Zhu, K.; Zhang, L.L.; Zhou, Y.W.; Liao, Q.X. Design and Experiment of Seed Flow Sensing Device for Precision Rapeseed Seed Meter. *Trans. Chin. Soc. Agric. Eng.* **2017**, *33*, 29–36. [CrossRef]
10. Chen, J.G.; Li, Y.M.; Qin, C.J.; Liu, C.L. Design and test of capacitive detection system for wheat seeding quantity. *Trans. Chin. Soc. Agric. Eng.* **2018**, *34*, 51–58. [CrossRef]
11. Mangus, D.L.; Sharda, A.; Flippo, D.; Strasser, R.; Griffin, T. Development of High-Speed Camera Hardware and Software Package to Evaluate Real-Time Electric Seed Meter Accuracy of a Variable Rate Planter. *Comput. Electron. Agric.* **2017**, *142*, 314–325. [CrossRef]
12. Ding, Y.C.; Wang, K.Y.; Liu, X.D.; Liu, W.P.; Chen, L.Y.; Liu, W.B.; Du, C.Q. Research progress of seeding detection technology for medium and smallsize seeds. *Trans. Chin. Soc. Agric. Eng.* **2021**, *37*, 31–41. [CrossRef]
13. Putra, B.T.W. New Low-Cost Portable Sensing System Integrated with on-the-Go Fertilizer Application System for Plantation Crops. *Measurement* **2020**, *155*, 107562. [CrossRef]
14. Sun, Y.J.; Jia, H.L.; Ren, D.L.; Yan, J.J.; Liu, Y. Experimental Study of Capacitance Sensors to Test Seed-Flow. *Appl. Mech. Mater.* **2013**, *347–350*, 167–170. [CrossRef]
15. Yilmaz, D.; Sagiroglu, H.C. Development of Measurement System for Grain Loss of Some Chickpea Varieties. *Measurement* **2015**, *66*, 73–79. [CrossRef]

16. Xie, C.; Yang, L.; Zhang, D.; Cui, T.; He, X.; Du, Z.; Xiao, T. A Signal Output Quantity (SOQ) Judgment Algorithm for Improving Seeding Quantity Accuracy. *Comput. Electron. Agric.* **2022**, *201*, 107321. [CrossRef]
17. Karimi, H.; Navid, H.; Besharati, B.; Behfar, H.; Eskandari, I. A Practical Approach to Comparative Design of Non-Contact Sensing Techniques for Seed Flow Rate Detection. *Comput. Electron. Agric.* **2017**, *142*, 165–172. [CrossRef]
18. Karimi, H.; Navid, H.; Besharati, B.; Eskandari, I. Assessing an Infrared-Based Seed Drill Monitoring System under Field Operating Conditions. *Comput. Electron. Agric.* **2019**, *162*, 543–551. [CrossRef]
19. Kumar, R.; Raheman, H. Detection of Flow of Seeds in the Seed Delivery Tube and Choking of Boot of a Seed Drill. *Comput. Electron. Agric.* **2018**, *153*, 266–277. [CrossRef]
20. Cay, A.; Kocabiyik, H.; Karaaslan, B.; May, S.; Khurelbaatar, M. Development of an Opto-Electronic Measurement System for Planter Laboratory Tests. *Measurement* **2017**, *102*, 91–95. [CrossRef]
21. Gergo, K.; Tamas, C.; Csaba, E.; Janos, S. Seed Counting Sensor and Method for Detecting Blockage of a Seed Conveying Pipe. U.S. Patent 10757856B2, 1 September 2020.
22. Sistemi Di Controllo per Macchine Agricole | MC Elettronica. Available online: https://www.mcelettronica.it/ (accessed on 3 March 2026).
23. Ding, Y.C.; Zhu, K.; Wang, K.Y.; Liu, X.D.; Du, C.Q. Development of monitoring device for medium and small size seed flow based on thin surface laser-silicon photocell. *Trans. Chin. Soc. Agric. Eng.* **2019**, *35*, 12–20. [CrossRef]
24. Ding, Y.C.; Wang, K.Y.; Du, C.Q.; Liu, X.D.; Chen, L.Y.; Liu, W.P. Design and experiment of high-flux small-size seed flow detection device. *Trans. Chin. Soc. Agric. Eng.* **2020**, *36*, 21–28. [CrossRef]
25. Ding, Y.C.; Yu, Q.L.; Dong, W.J.; Xu, C.B.; Zhang, W.X. Development of the solar-powered detection device for high-speed seeding seed flow of oil rape. *Trans. Chin. Soc. Agric. Eng.* **2025**, *41*, 83–93. [CrossRef]
26. Xu, C.B.; Liu, J.Y.; Su, Q.M.; Jin, W.; Wang, D.H.; Wang, W.C.; Ding, Y.C. Design and experiment of the wheat seed flow multi-channel parallel detection device with thin-surface light refraction. *Trans. Chin. Soc. Agric. Eng.* **2022**, *38*, 81–91. [CrossRef]
27. Wang, Z.M.; Pei, J.; He, J.; Zhang, M.H.; Yang, W.W.; Luo, X.W. Development of the sowing rate monitoring system for precision rice hill-drop drilling machine. *Trans. Chin. Soc. Agric. Eng.* **2020**, *36*, 9–16. [CrossRef]
28. Jiang, M.; Liu, C.L.; Du, X.; Dai, L.; Huang, R.B.; Yuan, H. Development of seeding rate detection system for precision and small amount sowing of wheat. *Trans. Chin. Soc. Agric. Eng.* **2021**, *37*, 51–58. [CrossRef]
29. Zhang, T.; Jiang, L.; Li, Z.D.; Xie, R.; Wang, W.W.; Chen, Y.X. Seed Flow Detection System of Optical Fiber Counting Rapeseed Precision Metering Device. *Trans. Chin. Soc. Agric. Mach.* **2023**, *54*, 64–74. [CrossRef]
30. Chen, L.Y. Design and Experiment of a Seeding Monitoring System for Precision Seeding. Master's Thesis, Huazhong Agricultural University, Wuhan, China, 2023.
31. Zhu, K. Design and Experiment of Photoelectric Sensor Device for Rapeseed and Wheat. Master's Thesis, Huazhong Agricultural University, Wuhan, China, 2020.
32. Wang, W.C. Design and Experiment of Wheat Seed Flow Multi-Channel Parallel Detection Device with Refracting Thin-Surface Light. Master's Thesis, Huazhong Agricultural University, Wuhan, China, 2023.
33. Liu, W.; Hu, J.; Zhao, X.; Pan, H.; Lakhiar, I.A.; Wang, W.; Zhao, J. Development and Experimental Analysis of a Seeding Quantity Sensor for the Precision Seeding of Small Seeds. *Sensors* **2019**, *19*, 5191. [CrossRef]
34. Qi, B.; Zhang, D.X.; Liu, Q.W.; Yang, L.; Shi, S.; Cui, T. Design and experiment of cleaning performance in a centralized pneumatic metering device for maize. *Trans. Chin. Soc. Agric. Eng.* **2015**, *31*, 21–27. [CrossRef]
35. Ju, X.T. Design and Research of a Mechanical Precision Seed Metering Device for Oil Seed Rape and Wheat. Master's Thesis, Northwest A&F University, Xianyang, China, 2025.
36. Ma, D.X. Design and Experiments of a Pneumatic Centrifugal Combined Precision Seed Metering Device for Wheat. Master's Thesis, Shandong Agricultural University, Tai'an, China, 2025.
37. Wang, Y.X.; Huang, S.T.; Zhang, W.Y.; Qi, B.; Zhou, X.Z.; Ding, Y.Q. Design and Experiment of Wheat Precision Seed Metering Device with Staggered Hook-tooth. *Trans. Chin. Soc. Agric. Mach.* **2024**, *55*, 142–153. [CrossRef]
38. Zhang, J.S. Circuit Design for NPN Silicon Triode Application. *Pract. Electron.* **2017**, 5–8. [CrossRef]
39. Wang, R.X.; Zhang, H.X.; Ji, J.T.; Wang, S.L.; Yu, Z.S.; Guo, Z.B. Design and Research on Wheat Precision Seeding System. *J. Chin. Agric. Mech.* **2026**, *47*, 184–191. [CrossRef]
40. Li, X.Y. Design of an On-Chip Integratable Opto-Coupler ChipBased on Silicon-Based BCD Process. Master's Thesis, University of Electronic Science and Technology of China, Chengdu, China, 2025.
41. Wu, Y.Q.; Zhang, J.K. Image Thresholding Based on Two-dimensional Histogram θθ-division and Maximum Between-cluster Deviation Criterion. *Acta Autom. Sin.* **2010**, *36*, 634–643.

Disclaimer/Publisher's Note: The statements, opinions and data contained in all publications are solely those of the individual author(s) and contributor(s) and not of MDPI and/or the editor(s). MDPI and/or the editor(s) disclaim responsibility for any injury to people or property resulting from any ideas, methods, instructions or products referred to in the content.